Does Topology Drive Fiber Polymerization?

Lihong Huang,*[,†] Joe Ping-Lin Hsiao,[‡] Camilla Powierza,[†] Russell M. Taylor, II,[‡] and Susan T. Lord[†]

[†]Department of Pathology and Laboratory Medicine and [‡]Department of Computer Science, University of North Carolina at Chapel Hill, Chapel Hill, North Carolina 27599, United States

S Supporting Information

ABSTRACT: We have developed new procedures to examine the early steps in fibrin polymerization. First, we isolated fibrinogen monomers from plasma fibrinogen by gel filtration. Polymerization of fibrinogen monomers differed from that of plasma fibrinogen. The formation of protofibrils was slower and the transformation of protofibrils to fibers faster for the fibrinogen monomers. Second, we used formaldehyde to terminate the polymerization reactions. The formaldehyde-fixed products obtained at each time point were examined by dynamic light scattering and transmission electron microscopy (TEM). The data showed the formaldehyde-fixed products were stable and representative of the reaction intermediates. TEM images showed monomers, short oligomers, protofibrils, and thin fibers. The amount and length of these species varied with time. Short oligomers were less than 5% of the molecules at all times. Third, we developed models that recapitulate the TEM images. Fibrin monomer models were assembled into protofibrils, and protofibrils were assembled into two-strand fibers using Chimera software. Monomers were based on fibrinogen crystal structures, and the end-to-end interactions between monomers were based on D-dimer crystal structures. Protofibrils assembled from S-shaped monomers through asymmetric D:D interactions were ordered helical structures. Fibers were modeled by duplicating a protofibril and rotating the duplicate 120° around its long axis. No specific interactions were presumed. The two protofibrils simply twisted around one another to form a fiber. This model suggests that the conformation of the protofibril per se promotes the assembly into fibers. These findings introduce a novel mechanism for fibrin assembly that may be relevant to other biopolymers.
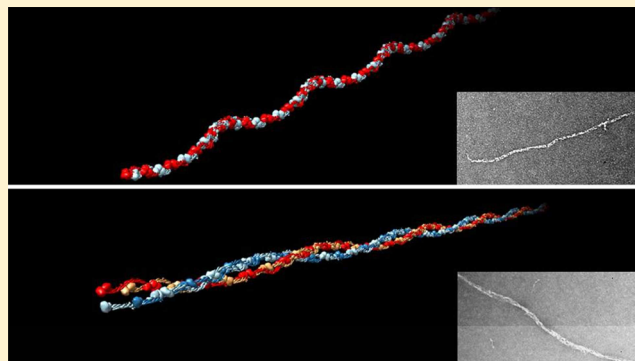
Many studies have provided insight into the mechanisms that promote polymerization of fibrin monomers into fibers. The classic light scattering studies of Hantgan and Hermans showed polymerization occurs in two steps: end-to-end polymerization of monomers into protofibrils and lateral association of protofibrils into fibers.[1] When the light scattering data were correlated with electron microscopy images, the two polymerization steps were identified as (1) the formation of half-staggered and double-stranded protofibrils and (2) a dramatic increase in fiber diameter.[2] Subsequent studies have confirmed this two-step model and the structure of the protofibril intermediate. Of note, modeling studies conducted by Weisel and co-workers also showed fibrin assembly and fibrin structure are kinetically determined.[3,4] In particular, kinetic analysis of images obtained by transmission electron microscopy (TEM) showed that reactions between oligomers are important for the polymerization of monomers into protofibrils.[4] More recently, Bernocco et al. studied the early stages of fibrin polymerization using stopped-flow multiangle laser light scattering technology.[5] They found the first step of polymerization is compatible with the formation of double-stranded, half-staggered semiflexible protofibrils of a limited length, and subsequently, such protofibrils assemble into fibers.

The molecular interactions that promote the polymerization of monomers into protofibrils are well-known.[6] Fibrin monomers contain three distinct structural regions: two distal D regions linked by coiled-coil connectors to one central E region. The D regions contain the polymerization sites known as holes "a", and the central E region contains two polymerization sites known as knobs "A". The knobs become exposed after thrombin cleaves fibrinopeptide A (FpA) from fibrinogen. Because the E region lies between two symmetric D regions, the reciprocal knob:hole, "A:a", interactions lead to a double-stranded protofibril with a half-staggered overlap between molecules in different strands. The end-to-end alignment of monomers in each protofibril strand forms the D:D interface. Even though the adjoined D regions are identical, crystallography studies have shown the D:D interface is asymmetric.

In contrast, the molecular interactions that promote assembly of protofibrils into fibers and the structures formed during this assembly remain unresolved. Several studies support a role for "B:b" knob:hole interactions and/or αC−αC interactions.[6,7]

Our experiments with recombinant fibrinogen variants indicate "B:b" interactions support protofibril formation and thereby enhance protofibril assembly,[8] while αC−αC interactions have an only modest influence on lateral aggregation.[9] Doolittle's group proposed a detailed theoretical model of fibrin formation.[10] In this model, two interactions support protofibril assembly: a primary interaction between γ-chains and a concomitant if subsidiary interaction between β-chains. These interactions were predicated on the intermolecular packing arrangements observed in crystal structures of fragment D from fibrinogen and the D-dimer isolated from cross-linked fibrin. These hypothetical possibilities have not been tested experimentally.

For the studies described here, we developed a novel method to "freeze" polymerization and provide "snapshots" of the different polymerization phases. We monitored thrombin-catalyzed polymerization of fibrinogen monomers, stopping the reactions at three time points: when protofibrils are forming, when protofibrils are growing, and when assembly of protofibrils into fibers is initiated. Because we stopped polymerization by the addition of formaldehyde, we were able to examine the polymer products by both dynamic light scattering (DLS) and transmission electron microscopy (TEM). Our DLS data showed that the formaldehyde-fixed products were stable and represented snapshots of the real-time DLS measurements. Our TEM data indicate fibrin monomers rapidly attached to protofibrils. We also developed three-dimensional models that accurately matched the structure of protofibrils and fibers seen by TEM in this study and in several other studies (for example, refs 4 and 11). These models were based on the crystal structures of fibrinogen and the D-dimer isolated from fibrin. They suggest that the shape of fibrinogen impacts the shape of the protofibril and the shape of the protofibril per se promotes the assembly of protofibrils into fibers. In contrast to previous models, no specific interactions were stipulated for the assembly of two protofibrils into a fiber.

■ EXPERIMENTAL PROCEDURES

Protein Preparation. Human plasma fibrinogen (Enzyme Research Laboratories, Inc.) was dialyzed overnight against 20 mM HEPES (pH 7.4) and 150 mM NaCl (HBS). Prior to polymerization studies, fibrinogen was diluted to 0.8 mg/mL in HBS with 1 mM $CaCl_2$. Fibrinogen concentrations were determined from A_{280}, using an extinction coefficient of 1.51 for a 1 mg/mL solution.

Gel Filtration Chromatography. Fibrinogen monomers were prepared as previously described.[9] Briefly, dialyzed fibrinogen was diluted to 8.0 mg/mL in HBS, filtered with a 0.22 μm GV DURAPORE centrifugal filter, and injected into a Superdex-200 column (GE Healthcare, Piscataway, NJ) equilibrated with HBS. Fractions (120 μL/tube) were collected and analyzed by DLS with a DLS plate reader (DynaPro, Waytt Technology, Santa Barbara, CA) and the absorbance at 280 with a Nanodrop spectrophotometer (Nanodrop 2000, Thermo Scientific, Wilmington, DE). The peak fractions containing fibrinogen monomers were combined together, adjusted to 0.8 mg/mL in HBS with 1 mM $CaCl_2$, and stored at 4 °C until they were used within 48 h.

Fibrinogen Polymerization. All buffers and fibrinogen samples were filtered (0.22 μm GV DURAPORE centrifugal filter) prior to use. Thrombin-catalyzed polymerization was monitored as the increase in the average hydrodynamic radius in a DLS plate reader. Reactions were conducted at ambient temperature with 0.4 mg/mL fibrinogen and 0.01 unit/mL human thrombin in HBS with 1 mM $CaCl_2$. Reactions were initiated by adding 60 μL of thrombin to 60 μL of fibrinogen and mixing thoroughly; the mixture was transferred into the plate reader wells. Polymerization was monitored for 60 min after the addition of thrombin. Data were collected every 10 s at 25 °C.

Formaldehyde "Stopped" Reactions. Reactions were conducted under the same conditions described in Fibrinogen Polymerization. Polymerization was initiated by mixing fibrinogen (0.8 mg/mL) with an equivalent volume of thrombin (0.02 unit/mL) in HBS with 1 mM $CaCl_2$ and immediately dividing the samples into three tubes (100 μL/tube). Twenty microliters of 0.5 M formaldehyde (prepared from paraformaldehyde, analyzed grade, Fisher Scientific[12]) was added at 5, 8, and 12 min, and the samples were rapidly mixed. The 0 min sample was prepared by mixing 50 μL of HBS buffer with 1 mM $CaCl_2$ with 50 μL of fibrinogen (0.8 mg/mL) and then adding 20 μL of 0.5 M formaldehyde. Samples were kept at room temperature for 30 min and 24 h and examined in the DLS plate reader.

Immunoblot Analysis of Fibrinogen. Polymerization was performed using the same conditions described in Formaldehyde "Stopped" Reactions. Reactions were stopped by adding SDS buffer under reduced conditions at 5, 8, and 12 min. The 0 min sample was prepared by adding SDS buffer under reduced conditions to fibrinogen. The samples were run on 8% polyacrylamide gels, transferred onto a nitrocellulose membrane, and developed with Aα chain specific monoclonal antibody Y-18 as previously described.[13] The blot was developed with ECL Western blotting detection reagents (GE Healthcare), and the bands were quantified using ImageJ (http://rsbweb.nih.gov/ij/).

Transmission Electron Microscopy (TEM). Formaldehyde-treated products were characterized by TEM. Formaldehyde-fixed polymer products at 0, 5, 8, and 12 min were diluted and transferred onto the 400 mesh, glow-discharged copper grids coated with Formvar/Carbon and then negatively stained with filtered 2% aqueous uranyl acetate essentially as described previously.[4] The samples were observed using a LEO EM-910 transmission electron microscope operating at 80 kV (Carl Zeiss SMT, Peabody, MA), and images were taken using a Gatan Orius SC1000 CCD camera with Digital Micrograph version 3.11.0 (Gatan, Inc., Pleasanton, CA) with a magnification of 100000×. We diluted samples as needed to obtain good TEM images with appropriate numbers of objects. We measured three aliquots of each sample, and the images are reproducible. All images were analyzed with ImageJ to measure the length and width of each object (monomer, oligomer, protofibril, and fiber). All the data were the average values of each species at different time points based on at least 10 images. The numbers of each species were counted by visual observation.

Modeling. We used UCSF Chimera (http://www.cgl.ucsf.edu/chimera/) to model the structures seen by TEM.[14] Molecular graphics images were produced using the UCSF Chimera package from the Resource for Biocomputing, Visualization, and Informatics at the University of California, San Francisco (supported by National Institutes of Health Grant P41 RR001081). The crystal structures of fibrinogen [Protein Data Bank (PDB) entries 3GHG and 1M1J] were used as a base for the monomer, and the D-dimer crystal structures (PDB entries 3H32 and 1FCZ) were used as a base

for the end-to-end interactions between monomers. Chimera allowed assembly of a composite model by producing multiple copies of a crystal structure, each of which could be moved and turned without disturbing the molecule's shape.

We assembled a protofibril beginning with the fibrin dimer. Two fibrinogens in the same orientation were juxtaposed visually to mimic the D:D interaction of the D-dimer. The juxtaposed molecules were then superimposed onto the D-dimer structures, and manual adjustments were made to minimize the differences. The transformation matrix between these two fibrinogens was repeated and used in a Chimera command to generate more monomers, attaching one monomer per iteration onto one end of the chain. This generated a helix structure. Small adjustments were made in the transformation matrix such that the chain more closely resembled the curvature seen in the TEM images. These steps established the transformation matrix of the D:D interaction in the dimer. The fibrin trimer was modeled from the dimer by positioning the third monomer in an inverted orientation such that the E region of the new monomer was centered over the D:D interface and the "a" sites in the new monomer were positioned as needed to form "A:a" interactions with the two E regions of the dimer. Each chain of the trimer was then elongated using the same transformation matrix that established the D:D interaction in the dimer.

We assembled a fiber from two protofibrils. One protofibril was duplicated, and the duplicate was rotated along the long axis to separate the two structures. A rotation of 120° generated a model that closely resembled the TEM images.

■ RESULTS

Polymerization was monitored by DLS. Using the DynaPro DLS plate reader, we determined that the average hydrodynamic radius of plasma fibrinogen was 16.1 nm. A histogram of these data (Figure 1A) showed a relatively wide size
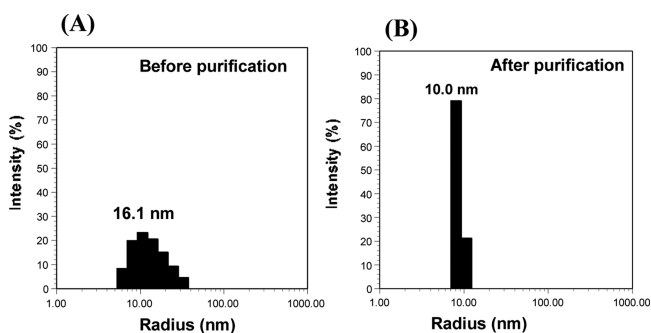

Figure 1. Hydrodynamic radius determined by DLS. The plots show the percent distribution of size in a representative fibrinogen sample (A) before and (B) after gel filtration chromatography. DLS was performed on samples of 0.4 mg/mL fibrinogen in HBS [20 mM HEPES and 150 mM NaCl (pH 7.4)] as described in Experimental Procedures.

distribution, indicating polydispersity. Following gel filtration chromatography, DLS analysis of the main peak (Figure 1B) showed a monodisperse sample whose hydrodynamic radius corresponded to that of the fibrinogen monomer (10.0 nm).[15] The hydrodynamic radius of monomeric fibrinogen remained constant for hours at ambient temperature, several days at 4 °C, and several months at −20 °C. Sodium dodecyl sulfate–polyacrylamide gel electrophoresis (SDS–PAGE) analysis

showed no degradation of the fibrinogen monomers during gel filtration (Figure S1 of the Supporting Information). Immunoblot analysis showed Factor XIII eluted with the fibrinogen monomers (Figure S2 of the Supporting Information).

We measured thrombin-catalyzed polymerization of fibrinogen before and after gel filtration by DLS; the data are shown in Figure 2. Both curves can be characterized by three stages: an
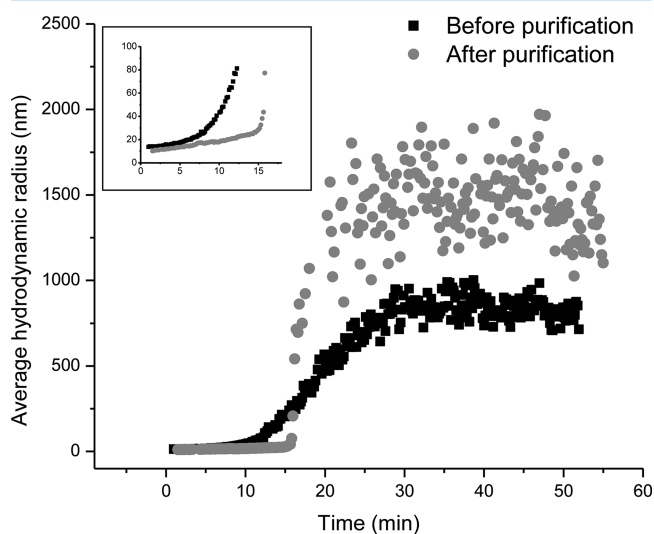

Figure 2. Thrombin-catalyzed polymerization monitored by DLS. Polymerization was initiated by adding thrombin (0.1 unit/mL) to fibrinogens (0.4 mg/mL) in HBS with 1 mM calcium, as described in Experimental Procedures. Polymer formation was measured as the average hydrodynamic radius as a function of time. The data are the average of three independent experiments with fibrinogen samples (■) before and (●) after gel filtration chromatography. The inset expands the first 15 min of the reactions.

early stage when the slope is relatively shallow, a midstage when the slope is steep, and a final stage when the curves reach a plateau. These stages reflect the steps of polymerization: the formation of protofibrils, the assembly of protofibrils into fibers, and the stable clot in which the fiber diameter remains constant. Both curves clearly showed all three stages, but their shapes were markedly different from one another. For polydisperse fibrinogen without gel filtration, the slope was comparatively low for 10 min. Thereafter, the slope became increasingly steeper until the average radius reached a plateau at 28 min. For monodisperse fibrinogen after gel filtration, the slope of the early stage was lower, around nearly zero. The midstage was initiated later, at 14 min, and the hydrodynamic radius increased dramatically. The curve reached a plateau sooner, around 22 min. Thus, the transformation of the protofibril to the final fiber took only 8 min for the monomer sample. In contrast, with polydisperse fibrinogen, the transformation of the protofibril to the fiber took ∼18 min. Finally, the diameter of fibers formed from fibrinogen monomers was much larger than the diameter of fibers formed from polydisperse fibrinogen. The average final radius for fibrinogen monomers (∼1500 nm) was approximately twice the average final radius for polydisperse fibrinogen (∼800 nm). Note that the average radius was determined by DynaPro software assuming a spherical particle, which of course is not the case for fibrin polymers or fibers. Nevertheless, the difference in the plateau values indicates the fibers formed from polydisperse

Table 1. Average Hydrodynamic Radii (nanometers) of Formaldehyde-Fixed Products[a]

samples analyzed by DLS	0 min	5 min	8 min	12 min
fixed products measured after 30 min	10.1 ± 0.1	18.6 ± 0.6	37.5 ± 3.9	100.4 ± 5.4
fixed products measured after 24 h	10.2 ± 0.2	18.7 ± 0.3	35.8 ± 6.1	93.4 ± 7.0
real-time polymerization	10.0 ± 0.1	13.0 ± 0.5	15.9 ± 0.5	20.5 ± 0.6

[a]Formaldehyde was added at different times before (0 min) and after addition of thrombin to fibrinogen. The radii for the formaldehyde-fixed products were determined 30 min or 24 h after the addition of formaldehyde. The real-time data correspond to those in Figure 2. The data are the mean radii ± the standard deviation from three experiments.
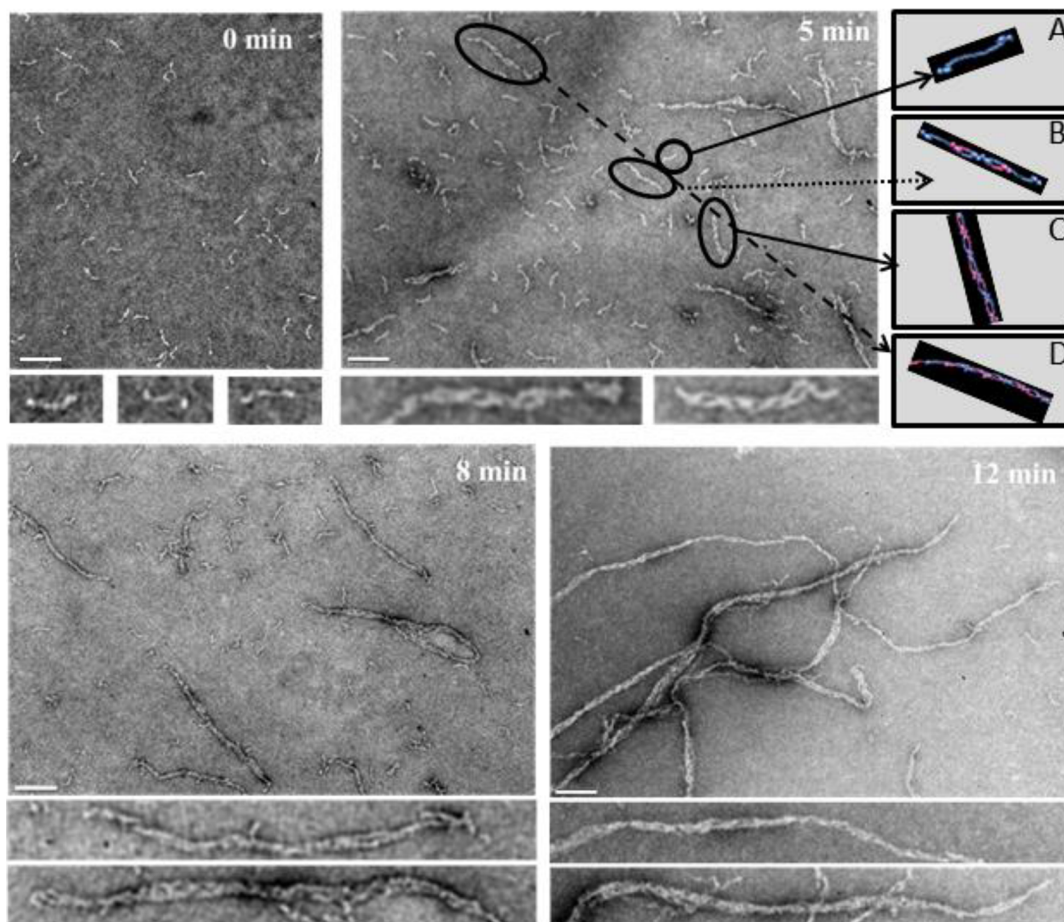

Figure 3. Transmission electron microscopy (TEM) images of formaldehyde-fixed products negatively stained with uranyl acetate. Polymerization was performed as described in the legend of Figure 2 and stopped by addition of formaldehyde prior to (0 min) or 5, 8, or 12 min after the addition of thrombin. A representative set of "fixed" polymer samples is shown. The scale bar is 100 nm, which is approximately twice the length of a fibrinogen monomer. Images below each field show individual structures on an expanded scale. Schematic representations of structures seen in 5 min are shown: (A) monomer, (B) trimer, (C) tetramer, and (D) hexamer.

samples are thinner than fibers formed from monodisperse samples. These data show that the aggregates present in plasma fibrinogen substantially influence the kinetics of polymerization. This conclusion is consistent with our recent studies that showed that polymerization was monitored by turbidity.[9] The physiological significance of our findings is unknown. Nevertheless, as discussed previously,[9] studies suggest that such aggregates indeed promote thrombotic disease. In the subsequent experiments reported here, we used only fibrinogen monomers.

Formaldehyde is able to "freeze" polymerization. We performed polymerization using the conditions described in the legend of Figure 2, adding formaldehyde to samples without thrombin and 5, 8, and 12 min after the addition of thrombin. As shown in Table 1, the average hydrodynamic radius of the

formaldehyde-treated samples increased with time, similar to the increase in radius seen in real time. We measured the radius of the fixed products 30 min and 24 h after the addition of formaldehyde and found these were the same. Thus, the addition of formaldehyde stops polymerization and "freezes" the polymers as stable products.

The hydrodynamic radius of fibrinogen (0 min) with formaldehyde was the same as that without formaldehyde. This result shows that the level of formation of intermolecular products by reaction of monomers with formaldehyde was low, below the detection limit of DLS. This result indicates that the addition of formaldehyde per se did not impact the structure or distribution of complexes. For example, the formaldehyde-fixed oligomers seen by TEM were formed by polymerization, not by formaldehyde-induced cross-linking. The hydrodynamic radius
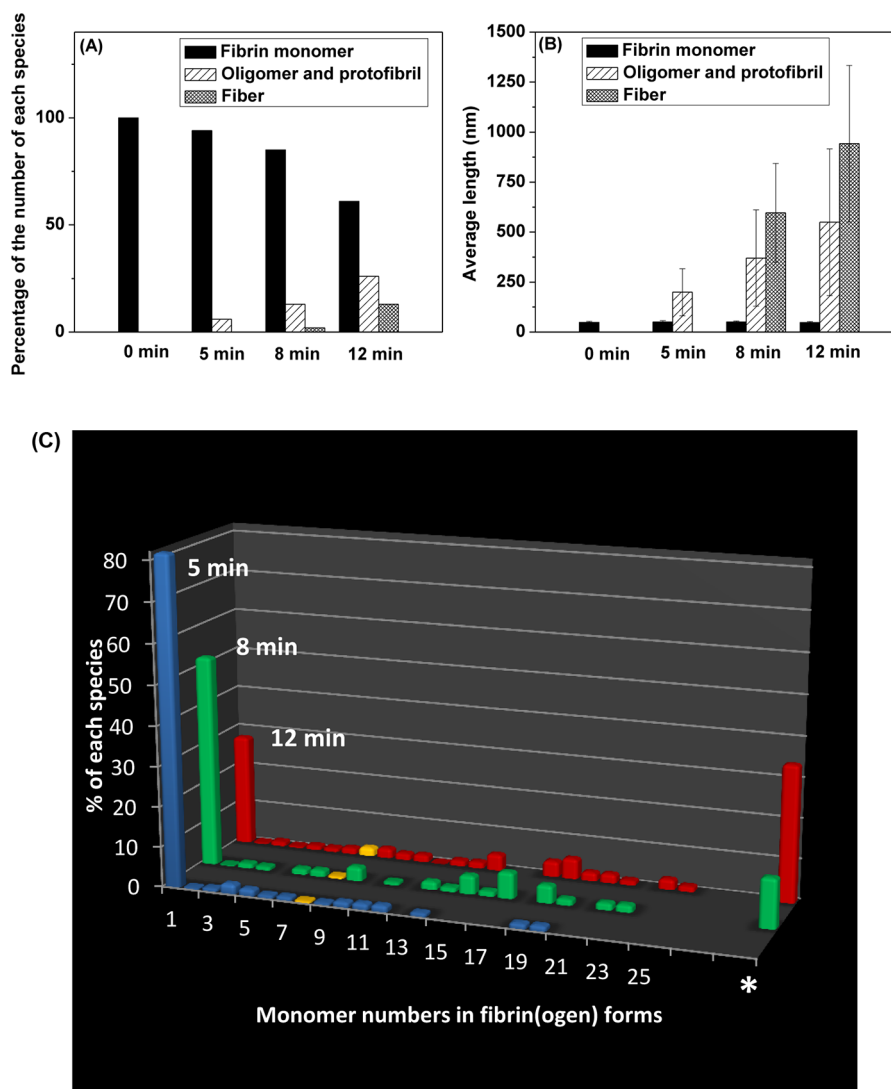
Figure 4. Quantitative assessment of the formaldehyde-fixed products. The histograms show the time-dependent analysis for (A) the percentage of each form (monomers, oligomers, and fibers) at each time, (B) the average length of each form (nanometers ± the standard deviation) at each time, and (C) the percentage of molecules found in each structure (measured as the number of monomers) at each time (5 min, blue; 8 min, green; 12 min, red); data for the smallest structures defined as protofibrils are colored yellow. The asterisk denotes molecules in long protofibrils containing more than 25 monomers and fibers.

of the formaldehyde-treated polymerization products was larger than the radius during real-time polymerization at the times of formaldehyde addition. For example, the hydrodynamic radius of the formaldehyde-fixed products at 5 min lies between the radii during real-time polymerization at 8 and 12 min. These data suggest that there is a 3−7 min delay to completely stop polymerization (see Table 1 and Figure 2). Considered altogether, the DLS data indicate that polymerization continues after the addition of formaldehyde, that formaldehyde links monomers that are within one polymer, and that once polymerization is arrested the formaldehyde-linked products are stable.

TEM provides clear snapshots of formaldehyde-fixed products. Representative TEM images of formaldehyde-fixed products (Figure 3) show the progression from monomers to oligomers, protofibrils, and fibers. The morphologies of individual monomers and monomers within each structure are evident. In particular, the half-staggered, double-stranded morphology of the protofibril was unmistakable (Figure 3, 5

min), and fibers of two or more protofibrils were clearly evident (Figure 3, 8 and 12 min). Our TEM images of protofibrils are similar to but apparently more uniform than those of Medved et al.[11] This uniformity may be a consequence of formaldehyde fixation prior to microscopy, the use of fibrinogen monomers, or both. For quantitative analysis of the images, we measured the length and width of each structure using ImageJ. We defined three structures by their width: monomers with a width between 4 and 6 nm, oligomers and protofibrils with a width between 8 and 13 nm, and fibers with a width greater than 13 nm. Before the addition of thrombin, only monomers were seen, as expected for fibrinogen purified by size exclusion chromatography. Short oligomers and protofibrils were observed when formaldehyde was added 5 min after thrombin. At 8 min, the oligomers and protofibrils increased in both size and number, and a small number of fibers appeared. At 12 min, more fibers were observed and the length of the longest fibers reached ∼2 μm. The TEM data also showed that even at the
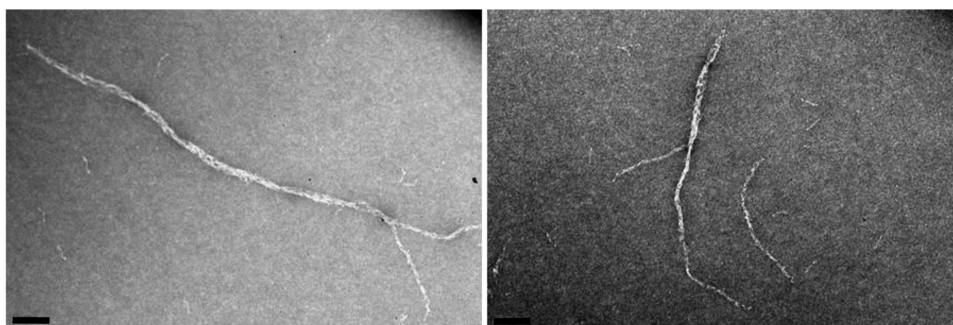
Figure 5. Special structure of the two-strand fibers. Two images were selected from the TEM images of formaldehyde-fixed products at 12 min. The scale bar is 100 nm.
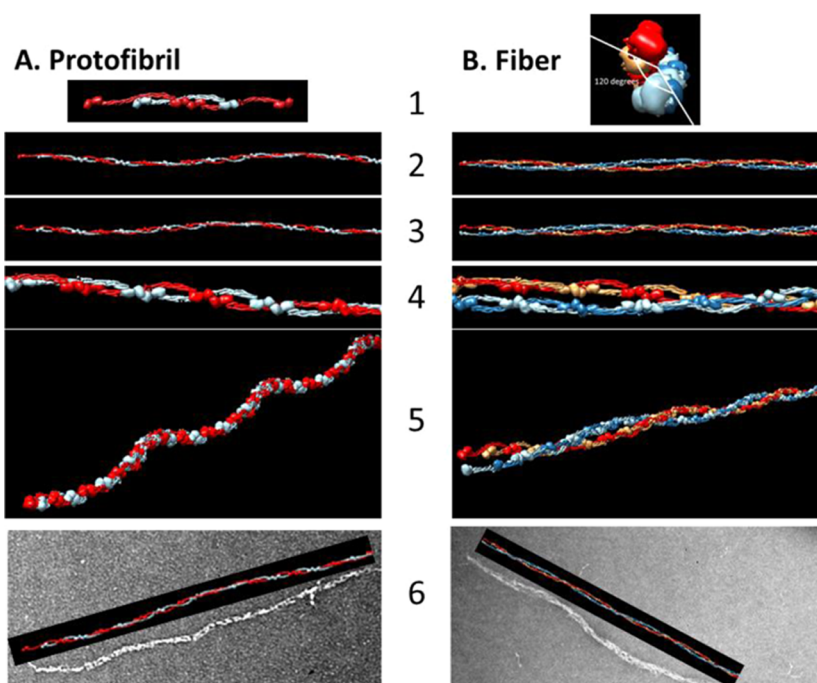

Figure 6. Models of (A) the protofibril and (B) the two-strand fiber. The models were generated with UCSF Chimera using the crystal structures of fibrinogen (PDB entry 1M1J) and the fibrin D-dimer (PDB entry 1FCZ). Two monomers (red) were joined to make a dimer by mimicking the D:D interface of the D-dimer. The trimer (A1) was made by adding a third monomer (blue) to align the "knobs" in the dimer with the "holes" in the third monomer. The double-stranded protofibril was formed by applying a transformation matrix that elongated the trimer by one monomer per iteration, as described in the text. The individual strands of the protofibril are colored blue and red. Four views are shown (A2−A5): front (A2), top (A3), close-up of the front (A4), and a perspective angle (A5). The model protofibril was scaled to and compared with a representative TEM protofibril (A6). The model of the two-strand fiber was developed by superimposing two protofibrils (one red, one blue) and rotating one of these 120° along its long axis (B1). Four views of the fiber are shown (B2−B5): front (B2), top (B3), close-up of the front (B4), and a perspective angle (B5). The model fiber was scaled to and compared with a representative TEM fiber (B6). Videos of these two models are provided in the Supporting Information.

earliest time (5 min), the polymerization products were relatively heterogeneous with a large distribution of sizes.

A quantitative assessment of the TEM images is shown in Figure 4. Figure 4A shows a histogram of the structures plotted as the percent of the three forms: monomers, oligomers including protofibrils, and fibers. Monomers decreased from 100% at 0 min to 94, 85, and 61% at 5, 8, and 12 min, respectively. Oligomers and protofibrils increased from 6% at 5 min to 13 and 26% at 8 and 12 min, respectively. Fibers first appeared at 8 min, increasing from 2% at 8 min to 13% at 12 min. We note that ∼77% of the fibers seen at 12 min were found in tangles, such as that shown in Figure 3. We found that the percent of each fibrin form did not change when the formaldehyde-stopped reaction mixtures were diluted prior to

analysis by TEM. Thus, the morphologic data, like the DLS data, showed the formaldehyde-fixed products are stable.

The average length of each form at different times is shown in Figure 4B. The length of the fibrin monomers remained ∼48 nm throughout. The length of oligomers and protofibrils increased continuously from ∼200 nm at 5 min to ∼550 nm at 12 min. Fibers increased in length from ∼600 nm at 8 min to ∼950 nm at 12 min. Considering all the TEM images, the average widths (±standard deviation) for monomers, oligomers including protofibrils, and fibers were 5.5 ± 1.3, 10.8 ± 2.2, and 22.3 ± 7.7 nm, respectively.

Surprisingly, only a few short oligomers were observed in these TEM images from 0 to 12 min. Figure 4C shows the data as the percent of fibrin(ogen) molecules found in each form at

each time. Note that the *Y*-axis in panel C differs from that in panel A; in panel C, the *Y*-axis is the percentage of total molecules that are monomers, while in panel A, the *Y*-axis is the percentage of each species out of the total number of objects. We found oligomers were less than 5% of the molecules at all times if we defined oligomers with eight or more monomers as protofibrils. As the reaction proceeded, the number and length of protofibrils increased. At 5 min, the longest protofibrils contained 20 monomers. Over time, an increasing number of molecules were involved in long protofibrils (>25 monomers) and thin fibers. At 12 min, long protofibrils and thin fibers constituted ~34% of all molecules. The very low representation of oligomers (<8 monomers) suggests that their lifetime is very short and that they quickly become protofibrils.

Most monomers observed in TEM are fibrinogen. To determine whether the monomers observed in the TEM images were fibrinogen or fibrin, we measured the fractional concentration of fibrinogen. We stopped polymerization by adding SDS buffer and analyzed the products on immunoblots developed with monoclonal antibody Y-18 that recognizes fibrinogen but not fibrin. The data (Figure S3 of the Supporting Information) showed that the concentrations of fibrinogen were 78, 63, and 31% of the total fibrin(ogen) molecules at 5, 8, and 12 min, respectively. These values were very similar to the relative concentrations of monomers shown in Figure 4C (82, 53, and 28%, respectively). These findings indicate that the monomers in the TEM images were almost all fibrinogen. The high concentrations of fibrinogen are expected in our reaction mixtures in which thrombin concentrations were low. Our findings indicate that once cleaved by thrombin, fibrin monomers are quickly conjugated with other fibrin forms.

Protofibrils twist to make fibers. Most interestingly, some images obtained after ≥8 min showed one special structure (Figure 5): fibers formed from two protofibrils twisted around each other. At one end, the protofibrils were separated, indicating they had not yet had a chance to form a complete fiber when polymerization was stopped by the addition of formaldehyde. These images suggest that the two protofibrils interacted at one end and twisted around each other step by step to form a two-stranded fiber.

A three-dimensional model recapitulates the architecture of the protofibrils and two-stranded fibers. We developed models for protofibrils and two-strand fibers using UCSF Chimera.[14] Each model was based on one crystal structure of fibrinogen and one crystal structure of the D-dimer. We used four crystal structures: the human fibrinogen structure (PDB entry 3GHG), the chicken fibrinogen structure (PDB entry 1M1J), and two human D-dimer structures (PDB entries 3H32 and 1FZC) that have different D:D interfaces. The four models developed from these structures were remarkably similar. In particular, all models showed the curved and twisted shapes that are described below. Considered together, the protofibril and fiber models indicate that the assembly of protofibrils into fibers is determined by the shape of the protofibril, which in turn is determined by the shape of the monomer. We present the model assembled from chicken fibrinogen (PDB entry 1M1J) using the D-dimer interface from the structure that mimics the "knob:hole" interactions found in human fibrin (PDB entry 1FCZ).

We modeled the protofibril starting with a trimer, as shown in Figure 6A. We first aligned the longitudinal interface between two monomers (colored red) to match the D:D interface in the D-dimer structure. We inserted the third (blue)

monomer based on the "A:a" "knob:hole" interactions that are known to be critical to protofibril formation. Because knob "A" is not visible in any crystal structure, one must make assumptions about the orientation of the knobs "A" in one monomer to the holes "a" in the adjacent monomer. Similar assumptions were made in a previous model of the protofibril.[10] We joined the knobs "A" from the central regions of the two monomers (Figure 6A1, red) with the holes "a" from the distal ends of a third monomer (blue), so this monomer faced the dimer. The trimer was expanded into a double-stranded protofibril in two stages, each of which repeatedly added one monomer at a time to the structure. In the first stage, red monomers were appended to form more D:D interactions. In each iteration, the left-hand monomer of the new D:D interaction was positioned adjacent to the right-hand monomer of the previous D:D interaction such that their relative positions and orientations matched those of the two original red monomers. Note that this added monomers onto the strand of the initial trimer and maintained the asymmetry that is found in the D:D interaction. In the second stage, we replicated blue monomers in the second protofibril strand and appended these one by one onto the original blue monomer using the relative transformation determined in stage 1. Thus, the second strand was identical to the first strand. Using this transformation repeatedly, it was a simple process to grow the double-stranded structures. As a consequence of this, all of the monomers' relative pairwise positions (and thus interactions) are identical throughout the protofibril.

Images of this model are shown in Figure 6A2−A5; videos showing rotation around the long axis and the center point of the model are available in the Supporting Information (Movies V1 and V2). When the structures are viewed from different perspectives, their shapes in the model vary; some segments appear as single strands, and some segments show gaps between the two strands. Of note, the strands in the model protofibril twist around one another (Figure 6A2−A4) with a pitch of two monomers, and the protofibril itself is spirally curved (Figure 6A5) with a pitch of seven monomers. The twist of the strands and the spiral curvature of the protofibril were present in all of our models, including those based on a different D:D interface (PDB entry 3H32) or on the human fibrinogen structure (PDB entry 3GHG). These modeling experiments indicate that the twist and the spiral curvature of the structure are inherent properties of a double-stranded protofibril that is uniformly assembled from the S-shaped fibrin monomers appended through asymmetric D:D interactions. These shapes are similar to the shapes of the protofibrils seen in our TEM images, as illustrated in Figure 6A6.

We also used the UCSF Chimera assembly tools to generate a model of a fiber constructed from two protofibrils. Images from this model are shown in Figure 6B; videos showing rotation around the long axis and the center point of the model are available in the Supporting Information (Movies V3 and V4). We duplicated the original protofibril, superimposed the two images, and then rotated the duplicate 120° around its long axis to separate the two strands as shown in Figure 6B1. The resultant structure was a two-strand fiber in which the two protofibrils twisted around one another with the same seven-monomer pitch as the protofibril (Figure 6B2−B5). It is not an accident that the two-strand fiber has the same pitch as a protofibril. Technically, the helix in the protofibril dictates the twist in the fiber. This simple modeling step suggests that the assembly of two protofibrils into a fiber reflects the twist and

spiral curvature of the protofibril. The model fiber is similar to the two-strand fibers seen in our TEM images, as illustrated in Figure 6B6.

■ DISCUSSION

Advantages of the "Formaldehyde-Fixed" Approach. In previous studies of fibrin structures formed during the early stages of polymerization, the reaction products were not fixed prior to TEM such that the experimental conditions might influence the outcome.[2,11] For example, oligomers could dissociate when reaction mixtures are diluted prior to application onto the microscopy grid. To overcome this potential flaw, we stopped the reactions by adding formaldehyde. We found the TEM images of the formaldehyde-fixed products were unchanged by dilution in buffer. DLS of the fixed products confirmed that formaldehyde stopped the reactions and showed that the formaldehyde-fixed products were stable. Thus, the TEM images reflect the morphology of the products present at the time of addition of formaldehyde. Our images are reminiscent of images of protofibrils and fibers whose reactions were arrested by dilution into 0.05 M ammonium acetate and immediately placed on the microscopy grid.[4] This morphological similarity indicates that formaldehyde treatment per se did not substantially alter the polymer structures.

Comparing the DLS of the fixed products to the DLS of real-time samples at the time of fixation suggests a time delay in stopping the reactions. Because DLS measures changes with time, it may be misleading to compare the real-time data, where the structures are not only moving but also changing with time, to those of the formaldehyde-stopped reactions, where the structures are stable. Nevertheless, we note that this time delay suggests the structures in the fixed samples are indeed different from those at the equivalent real time. One might anticipate this difference if the larger structures were more likely to be fixed by formaldehyde. This suggests that the smaller structures are very short-lived relative to the time needed to covalently link the monomers. The tangled structure seen at 12 min in Figure 3 should also be considered when comparing the real-time DLS to that of the fixed samples. Such large structures would have a disproportionate influence on the value of the average DLS, as such structures would be less mobile than the same structures moving independently. We conclude that formaldehyde-fixed approach provides an accurate representation of the structures formed early in polymerization.

Implications of the Quantitative TEM Results. The data shown in Figure 4C differ from similar histograms reported by Weisel et al.[4] These differences could all arise from differences in experimental conditions. We saw a larger fraction of monomers, mostly fibrinogen, at all times, consistent with the low thrombin concentration (0.25 unit/mg of fibrinogen) used here. In contrast, the monomer peak in the previous study is undoubtedly fibrin, as the thrombin concentration was high (100 units/mg of fibrinogen). Thus, the previous histograms provide a more accurate estimate of the lifetime of the fibrin monomer. We saw a small and relatively uniform fraction of oligomers and protofibrils; they report dips and peaks indicating accumulation of specific intermediates. Weisel et al. used plasma fibrinogen in their studies. Our gel filtration data suggest histograms of this fibrinogen would show oligomers. Thus, the oligomer intermediates that change during the reaction could reflect the presence of larger species in the starting material. We saw no evidence of stable oligomers. This finding indicates that specific intermediates do not accumulate during thrombin-catalyzed polymerization of monomeric fibrinogen. Lastly, our histogram peaks are shifted to the right, indicating assembly into large structures occurred more rapidly in our experiments. This difference would be anticipated from the DLS data (Figure 2). The DLS curves show larger species accumulate earlier during polymerization of plasma fibrinogen relative to polymerization of fibrinogen monomers. Irrespective of these differences, both analyses showed oligomers were quickly assembled into protofibrils and fibers.

In recent studies, Weisel and his colleagues have compared quantitative TEM data with structures visualized by spinning disc confocal microscopy. These complementary approaches allowed the visualization of real-time polymerization of hydrated samples alongside the high-resolution characterization of the structures present at specific times. These studies used kinetic conditions similar to ours, 0.07 unit of thrombin/mg of fibrinogen, though with plasma fibrinogen. We compared the snapshots at our three time points to the three earliest time points in this study where the percents of monomers are nearly the same: 81, 52, and 28% for our studies and 78, 55, and 40% for theirs, respectively. This comparison shows the results from the two studies are quite similar. At the earliest time, both samples were heterogeneous though more so in our sample. We saw small amounts ($\leq 2\%$) of every species, monomer through dodecamer, plus a few larger, while they saw a decreasing fraction with increasing size, i.e., fewer trimers than dimers. They did not see oligomers of five, six, or seven monomers, while we saw these species in essentially all our samples. In both studies, fibers were first observed at the second time, and the fractions of fibers were similar, ~10%. The spinning disc confocal microscopy data confirmed that fibers were present, but not the primary structure at this time. In both studies, the fraction of fibers increased and the fraction of protofibrils decreased when comparing the third time to the second time. This finding suggests that the assembly of protofibrils into fibers was the dominant process when the third sample was obtained. That is, the fibers are growing in diameter more rapidly than protofibrils are forming. Both analyses show a small fraction of oligomers are present throughout these times, indicating that these oligomers assemble rapidly and that they add to both protofibrils and fibers. Neither set of data could distinguish whether oligomers add to fibers by assembling alongside or elongating the protofibrils existing within the fibers.

Implications of Modeling. We developed models based on the S-shape of fibrinogen and the asymmetric D:D interface. We assembled a trimer and added monomers to build a half-staggered, double-stranded protofibril. Examination of the model protofibril illustrates that the varying TEM images seen here and in published reports can arise from different perspectives of the same structure. The constraints used in building this model induced a twist of one chain around the second. Several early studies have also noted a twisted structure. Indeed, a hint of twisting was first perceived more than 40 years ago.[16] In 1990, Medved et al.[17] published remarkable TEM images that clearly showed crossover points of the chains within a protofibril as expected if the chains twist around one another. Our model also showed the twisted strands form a spiral structure. This suggests that protofibrils are ordered helical structures. Both the twisted strands and the spiral structure arise from the asymmetric D:D interface that is evident in almost all crystal structures. Indeed, the one variant fibrinogen,

γN308 K, whose crystal structure showed a symmetric D:D interface does not form stable protofibrils.[18]

We then assembled a fiber by simply rotating one of two identical, superimposed protofibrils. The similarity between the model fiber and the fibers seen in TEM leads us to hypothesize that the modeling recapitulates the assembly of two protofibrils into a fiber. The modeling suggests that it is the conformation of the protofibril per se, both its twisted surface and its spiral curvature, that promotes the assembly. The protofibril surfaces must be compatible, but specific interactions between protofibrils were not stipulated. The structures shown in Figure 5 are consistent with this model: the two protofibrils assembled from one end, twisting around one another to form the two-protofibril fiber. The assembly was stopped by the addition of formaldehyde before the two protofibrils were fully annealed, forming the Y-shaped structures.

Our model shows the protofibril and the fiber have the same helical pitch. Indeed, the helical pitch of the protofibril, seven monomers, sets the helical pitch of the fiber. In 1987, Weisel et al. observed a similar helical structure in fibers and measured the average pitch as 1930 ± 280 nm, equivalent to 43 ± 6 monomers.[19] This pitch is much larger than the pitch of our model and the structures shown in our TEM images. The difference may arise from the conditions of polymerization, as these conditions will affect the morphology of the fibers. The earlier studies were completed at much higher thrombin and fibrinogen concentrations. Further, it is possible that addition of formaldehyde preserved the steeper pitch observed in our fibers.

All previous models of the assembly of protofibrils into fibers stipulate specific intermolecular interactions. Assembly occurs after the protofibrils reach a specific length, approximately 16 monomers. This observation suggests that multiple weak interactions between protofibrils are required to initiate assembly. As FpB release correlates with the growth in fiber diameter, "B:b" interactions were the first implicated in assembly.[20] However, even this early study showed "B:b" interactions were not required. Fibers were formed when fibrinogen was cleaved by snake venoms that released only FpA, such that "B:b" interactions were not present. Subsequent studies resolve this apparent inconsistency.[21] These suggest the release of FpB per se and "B:b" interactions enhance the formation of protofibrils and consequently enhance assembly of protofibrils into fibers. Many studies have shown the αC domains influence polymerization and fiber diameter.[22] Gorkun et al. correlated electron microscopy and turbidity studies using fibrinogen preparations missing one or both of these domains. These experiments led to an appealing model in which the αC regions interact intramolecularly in fibrinogen but intermolecularly in fibrin. These intermolecular interactions promote assembly. Studies with recombinant fibrinogen lacking the αC regions indicate these regions do indeed influence polymerization, but the effect is modest.[9,23,24] Without αC, the fiber diameter was slightly smaller, indicating the assembly of protofibrils was inhibited but not eliminated. Thus, like the "B:b" interactions, the αC:αC interactions were not required for the assembly of protofibrils.

These findings naturally evoke the hypothesis that two, or more, types of specific interactions work together to support the assembly of protofibrils into fibers. This hypothesis has been tested with recombinant fibrinogens that combined the loss of the αC domain with other changes that influence polymerization: BβD398A and γE132A (L. Huang, L. Ping, O.

V. Gorkun, and S. T. Lord, unpublished data). The individual variants showed little or no change in turbidity that could reflect changes in the assembly of protofibrils, while the double mutations (αC/BβD398A and αC/γE132A) show only modest changes in turbidity. These data show that the loss of both αC:αC and "B:b" interactions, or other pairs of interactions, did not eliminate the assembly of protofibrils into fibers. Perhaps an additional, unidentified specific interaction is also required. We examined the interface between the two protofibrils (orange and blue) in our model fiber. We used UCSF Chimera to determine the point of closest approach and identified the atom pair: the side chain oxygen for chain residue Thr 358 and the backbone amide for chain reside Glu 270. Thr 358 lies within one half of the primary interacting site, residues 350−360, in the molecular model of fibrin assembly proposed by Doolittle's group.[10] Residue Glu 270, however, is not within the proposed complementary segment of residues 370−380. Thus, assembly of the protofibrils in our model does not recapitulate the previously proposed interface. For those interested in additional molecular details, our model can be accessed via the CISMM web server (http://cismm.cs.unc.edu/wp-content/uploads/2014/10/fiber_pdb.zip).

The only variant fibrinogen whose protofibrils appear to be unable to assemble into fibers is a hybrid molecule in which the normal human αC domain was replaced with the analogous chicken αC domain.[25] Light scattering studies indicate that protofibrils formed with this hybrid; however, fibers did not form, and no fibrin clot was evident. It is difficult to interpret these data. TEM studies showed the hybrid fibrinogen structure differs from that of normal fibrinogen. Approximately 89% of the hybrid molecules are U-shaped or complicated shaped under conditions where 90% of normal fibrinogen is S-shaped (L. Huang, L. Ping, C. Powierza, O. V. Gorkun, and S. T. Lord, unpublished data). This observation supports our model in which the S shape of fibrinogen has a critical role in polymerization. It should be noted, however, that natural chicken fibrinogen is slow to polymerize when tested under similar conditions. The natural protein does form a fibrin clot, although one with relatively thin fibers (L. Huang, L. Ping, O. V. Gorkun, and S. T. Lord, unpublished data). These studies suggest that αC regions do have a role in fiber assembly, although in this case, an inhibitory role.

Alternatively, the long-held premise that protofibril assembly requires specific interactions may be incorrect. We propose a model in which assembly of protofibrils is driven by topology rather than multiple specific interactions. There is no clear precedence for such a conformation-driven assembly. A critical role for conformation has been suggested in two earlier studies that also examined electron microscopy images. In a study with modified fibrin, Wade et al. proposed that the protofibril has a tendency to twist and assemble with other protofibrils to form an ordered twisted fibril.[26] They noted that tensions in the right-handed twist of the protofibril are partially relieved when it assembles into a left-handed coil. In other words, the authors proposed the driving force for fiber assembly is the tension introduced by the twist in the protofibril. One year later, Ferry's group examined images that showed branching junctions in fine clots.[27] These authors suggest the strength of the junctions is enhanced because of topological constraints provided by twisting rather than the noncovalent interactions between protofibrils. Thus, these authors limit the role of conformation to the branch points. We propose that the spiral conformation of the twisted protofibril drives assembly of protofibrils into

fibers. We note that the spiral of the model protofibril is right-handed while the coil of the model fiber is left-handed. Thus, tension in the protofibril could be reduced by assembly into the fiber. This discussion suggests a possible precedence for our model, the assembly of α-helices into coiled coils. This assembly is also dependent on conformation. Again, right-handed structures, the α-helices, are assembled in a left-handed coil. We also note a recent study that may be relevant to our model. This study suggests the "A:a" interactions could provide stability to a protofibril structure under tension. The data showed "A:a" interactions exhibit "catch-slip" kinetics, indicating that these interactions exist in two states.[28] Perhaps the assembly of monomers into protofibrils is supported by the "catch" bond, providing stability to a right-handed, twisted, spiral. During subsequent assembly into a left-handed fiber, the "A:a" interaction "slips" into the alternative state that is stable within the fiber. This idea is highly speculative. Nevertheless, it seems reasonable to propose that the "A:a" interactions in protofibrils differ from those in fibers.

In conclusion, our data are consistent with many previous studies. They show protofibrils are twisted structures and protofibril assembly into fibers can lead to fiber branching. In contrast, our model is unique. This model shows protofibrils are ordered helical structures and suggests that the assembly of protofibrils into fibers is driven by geometry rather than specific intermolecular interactions.

■ ASSOCIATED CONTENT

Ⓢ Supporting Information

Nonreduced SDS−PAGE gel results of fibrinogen before and after purification (Figure S1), immunoblot analysis of fibrinogen fractions from size exclusion chromatography (Figure S2), immunoblot analysis of the fibrinogen monomer at different polymerization time points to quantify the remaining monomers (Figure S3), and rotation videos of the protofibril and fibers around the long axis and the center point of the models (Movies S1−S4). This material is available free of charge via the Internet at http://pubs.acs.org.

■ AUTHOR INFORMATION

Corresponding Author

*Lineberger Cancer Center, University of North Carolina at Chapel Hill, CB# 3290, Chapel Hill, NC 27599. E-mail: lihongh@email.unc.edu. Telephone: (919) 518-7699. Fax: (919) 962-5467.

Author Contributions

L.H. designed and performed experiments, analyzed data, prepared figures, and wrote the manuscript. J.P.-L.H. performed the modeling experiment and wrote the manuscript. C.P. performed experiments, analyzed the data, and modified the manuscript. R.M.T. supervised the experiment design and performance of modeling part and wrote the paper. S.T.L. supervised the study, designed experiments, analyzed data, and wrote the manuscript.

Notes

The authors declare no competing financial interest.

■ ABBREVIATIONS

TEM, transmission electron microscopy; DLS, dynamic light scattering; OD, optical density; FpA, fibrinopeptide A; HBS, 20 mM HEPES (pH 7.4) and 150 mM NaCl; SDS, sodium dodecyl sulfate.

■ REFERENCES

(1) Hantgan, R. R., and Hermans, J. (1979) Assembly of fibrin. A light scattering study. *J. Biol. Chem. 254*, 11272−11281.

(2) Hantgan, R., Fowler, W., Erickson, H., and Hermans, J. (1980) Fibrin assembly: A comparison of electron microscopic and light scattering results. *Thromb. Haemostasis 44*, 119−124.

(3) Weisel, J. W., and Nagaswami, C. (1992) Computer modeling of fibrin polymerization kinetics correlated with electron microscope and turbidity observations: Clot structure and assembly are kinetically controlled. *Biophys. J. 63*, 111−128.

(4) Weisel, J. W., Veklich, Y., and Gorkun, O. (1993) The sequence of cleavage of fibrinopeptides from fibrinogen is important for protofibril formation and enhancement of lateral aggregation in fibrin clots. *J. Mol. Biol. 232*, 285−297.

(5) Bernocco, S., Ferri, F., Profumo, A., Cuniberti, C., and Rocco, M. (2000) Polymerization of rod-like macromolecular monomers studied by stopped-flow, multiangle light scattering: Set-up, data processing, and application to fibrin formation. *Biophys. J. 79*, 561−583.

(6) Lord, S. T. (2007) Fibrinogen and fibrin: Scaffold proteins in hemostasis. *Curr. Opin. Hematol. 14*, 236−241.

(7) Weisel, J. W. (2005) Fibrinogen and fibrin. *Adv. Protein Chem. 70*, 247−299.

(8) Mullin, J. L., Gorkun, O. V., and Lord, S. T. (2000) Decreased Lateral Aggregation of a Variant Recombinant Fibrinogen Provides Insight into the Polymerization Mechanism. *Biochemistry 39*, 9843−9849.

(9) Huang, L., and Lord, S. T. (2013) The isolation of fibrinogen monomer dramatically influences fibrin polymerization. *Thromb. Res. 131*, e258−e263.

(10) Yang, Z., Mochalkin, I., and Doolittle, R. F. (2000) A model of fibrin formation based on crystal structures of fibrinogen and fibrin fragments complexed with synthetic peptides. *Proc. Natl. Acad. Sci. U.S.A. 97*, 14156−14161.

(11) Medved, L., Ugarova, T., Veklich, Y., Lukinova, N., and Weisel, J. (1990) Electron microscope investigation of the early stages of fibrin assembly. Twisted protofibrils and fibers. *J. Mol. Biol. 216*, 503−509.

(12) Kiernan, J. (2000) Formaldehyde, formalin, paraformaldehyde and glutaraldehyde: What they are and what they do. *Microsc. Today 1*, 8−12.

(13) Gorkun, O. V., Veklich, Y. I., Weisel, J. W., and Lord, S. T. (1997) The conversion of fibrinogen to fibrin: Recombinant fibrinogen typifies plasma fibrinogen. *Blood 89*, 4407−4414.

(14) Goddard, T. D., Huang, C. C., and Ferrin, T. E. (2005) Software extensions to UCSF chimera for interactive visualization of large molecular assemblies. *Structure 13*, 473−482.

(15) Cardinali, B., Profumo, A., Aprile, A., Byron, O., Morris, G., Harding, S. E., Stafford, W. F., and Rocco, M. (2010) Hydrodynamic and mass spectrometry analysis of nearly-intact human fibrinogen, chicken fibrinogen, and of a substantially monodisperse human fibrinogen fragment X. *Arch. Biochem. Biophys. 493*, 157−168.

(16) Krakow, W., Endres, G. F., Siegel, B. M., and Scheraga, H. A. (1972) An electron microscopic investigation of the polymerization of bovine fibrin monomer. *J. Mol. Biol. 71*, 95−103.

(17) Medved, L., Ugarova, T., Veklich, Y., Lukinova, N., and Weisel, J. (1990) Electron microscope investigation of the early stages of fibrin assembly. Twisted protofibrils and fibers. *J. Mol. Biol. 216*, 503−509.

(18) Bowley, S. R., Okumura, N., and Lord, S. T. (2009) Impaired protofibril formation in fibrinogen γ N308K is due to altered D:D and "A:a" interactions. *Biochemistry 48*, 8656−8663.

(19) Weisel, J. W., Nagaswami, C., and Makowski, L. (1987) Twisting of fibrin fibers limits their radial growth. *Proc. Natl. Acad. Sci. U.S.A. 84*, 8991−8995.

(20) Blombäck, B., Hessel, B., Hogg, D., and Therkildsen, L. (1978) A two-step fibrinogen−fibrin transition in blood coagulation. *Nature 275*, 501−505.

(21) Lord, S. T. (2007) Fibrinogen and fibrin: Scaffold proteins in hemostasis. *Curr. Opin. Hematol. 14*, 236−241.

(22) Weisel, J. W., and Medved, L. (2001) The structure and function of the αC domains of fibrinogen. *Ann. N.Y. Acad. Sci. 936*, 312−327.

(23) Gorkun, O. V., Henschen-Edman, A. H., Ping, L. F., and Lord, S. T. (1998) Analysis of Aα251 fibrinogen: The αC domain has a role in polymerization, albeit more subtle than anticipated from the analogous proteolytic fragment X. *Biochemistry 37*, 15434−15441.

(24) Collet, J.-P., Moen, J. L., Veklich, Y. I., Gorkun, O. V., Lord, S. T., Montalescot, G., and Weisel, J. W. (2005) The αC domains of fibrinogen affect the structure of the fibrin clot, its physical properties, and its susceptibility to fibrinolysis. *Blood 106*, 3824−3830.

(25) Ping, L., Huang, L., Cardinali, B., Profumo, A., Gorkun, O. V., and Lord, S. T. (2011) Substitution of the human αC region with the analogous chicken domain generates a fibrinogen with severely impaired lateral aggregation: Fibrin monomers assemble into protofibrils but protofibrils do not assemble into fibers. *Biochemistry 50*, 9066−9075.

(26) Hewat, E. A., Tranqui, L., and Wade, R. H. (1983) Electron microscope structural study of modified fibrin and a related modified fibrinogen aggregate. *J. Mol. Biol. 170*, 203−222.

(27) Müller, M. F., Ris, H., and Ferry, J. D. (1984) Electron microscopy of fine fibrin clots and fine and coarse fibrin films. Observations of fibers in cross-section and in deformed states. *J. Mol. Biol. 174*, 369−384.

(28) Litvinov, R., and Weisel, J. (2013) Shear strengthens fibrin: The knob−hole interactions display "catch-slip" kinetics. *J. Thromb. Haemostasis 11*, 1933−1935.